International Journal of Control and Automation
Vol.7, No.7 (2014), pp. 203-216
http://dx.doi.org/10.14257/ijca.2014.7.7.17

Proportional-Integral Sliding Mode Control for Trajectory Tracking and Vibration Control of a Flexible Single Link Manipulator

Mohammed Rachidi and Badr Bououlid Idrissi

Moulay Ismaïl University, Ecole Nationale Supérieure d'Arts et Métiers, BP 4024, Marjane II, Beni Hamed, 50000, Meknès, Morocco
morachidi@yahoo.fr, badr.bououlid@gmail.com

Abstract

This paper presents investigations into the development of a Proportional-Integral Sliding Mode Control (PI-SMC) for trajectory tracking and vibration control of a flexible single link manipulator. The motor at the single rotating joint is the control actuator. Two SMC control laws are reviewed. The classical discontinuous control based on the signum function and a modified control law where the servomotor output voltage depends on the instantaneous values of the states. The selection of the discontinuity gain is reviewed for exact model (certain case) as well as when the parameter variations are present (uncertain case). To prove the reaching condition, we use the Lyapunov stability criteria. It is proven that this design is equivalent to a full state feedback with its steady state motion constrained to the sliding hyper-surfaces. Simulation results of the response of the flexible manipulator with both controllers are presented. The performances of the control schemes are examined for input tracking capability, level of vibration reduction and time response specifications. A comparative assessment of both control techniques shows the effectiveness of the second control law and its invariance to so-called matched uncertainty.

Keywords: *Vibration reduction, flexible manipulator, sliding mode control, model uncertainties*

1. Introduction

Current generation of industrial robots need to be rigid to achieve precise control with today's established control methods. Rigidity, however, necessitates massive construction, that results in slow operation, low load to weight ratio and high energy consumption. For faster response time, manipulators must be made with thin and light weight links that eventually lead to links flexibility. Using light weight links manipulators in industry has many advantages. Indeed, flexible links manipulators have higher speed, higher load to weight ratio, low energy consumption, lower overall cost and higher mobility.

Control systems for light weight flexible arms, however, have to overcome more problems. Because of links flexibility and hence arms vibration, precise position control is much more difficult [1-4]. Also, a flexible arm is basically an under-actuated nonlinear system of infinite order. But due to the limitations of nowadays control processors, it is common to approximate a flexible arm by a finite order system. In this study, the assumed modes method is used and only the first two vibration modes are considered. Furthermore, in a single link manipulator arm, such as the one that will be modeled, the tip sensor and the actuator are located at the two ends of the arm. Such a

ISSN: 2005-4297 IJCA

non-collocated sensor/actuator configuration yields to some control problems because of the non-minimum phase characteristics of the system [4-6].

To solve these problems, good controller designs are needed. A good controller has to be simple, practical, easy to implement and able to achieve good control performance. Variable structure sliding mode control is a good choice for this design because it has offered control engineers new possibilities for improving the performance of control in comparison to fixed structure systems [7, 13]. An important possibility is to improve the performance by combining properties of the structures at the two sides of the switching line. We can also solve the conflict between static accuracy and speed of response. Indeed, it is possible to split the transient movement into two independent phases: a brief motion which brings the system's state to the beginning of the sliding mode and achieves high rate of decrease in the absolute value of the error, and a second phase characterized by rapid damped oscillations. The good qualities of the variable structure sliding mode control are the reasons why we focus on applying this theory.

This paper presents investigations into the development of a Proportional-Integral Sliding Mode Control (PI-SMC) for trajectory tracking and vibration control of a flexible single link manipulator [8-12]. The flexible link is modeled as an Euler-Bernoulli beam and we apply Lagrange equations to derive the state-space model. To illustrate the surface design techniques, the original system is transformed to "regular form". We show that the problem of designing a system with desirable properties in the sliding mode can be regarded as a state feedback design problem. The selection of the discontinuity gain is reviewed in the case of exact model (certain case) as well as when the parameter variations are present (uncertain case). To prove the reaching condition, we use the Lyapunov stability criteria. In the uncertain case, it turns out when using the classical signum function, that bounds on values of the state vector must be known. The reaching condition in this case leads to high value of the discontinuity gain which has the effect of amplifying chattering and cause significant fatigue of the actuators. To keep the discontinuity gain independent of the states, a modified SMC control law is proposed. Simulation results show that the discontinuity gain can be set to its minimal value imposed by the specified convergence speed. A comparative assessment of the control techniques shows the effectiveness of the second control law and its invariance to so-called matched uncertainty.

2. Mathematical Model

2.1. Flexible Arm Modeling

The flexible arm is treated as a Bernoulli beam. It is fixed to the rotor of a servomotor and rotates in a horizontal plane. The effect of gravity and internal damping are negligible.

In the Figure 1, (OXYZ) denotes the fixed reference frame; (Oxyz) is a rotating coordinate system with basis vectors $(\vec{i}, \vec{j}, \vec{k})$.

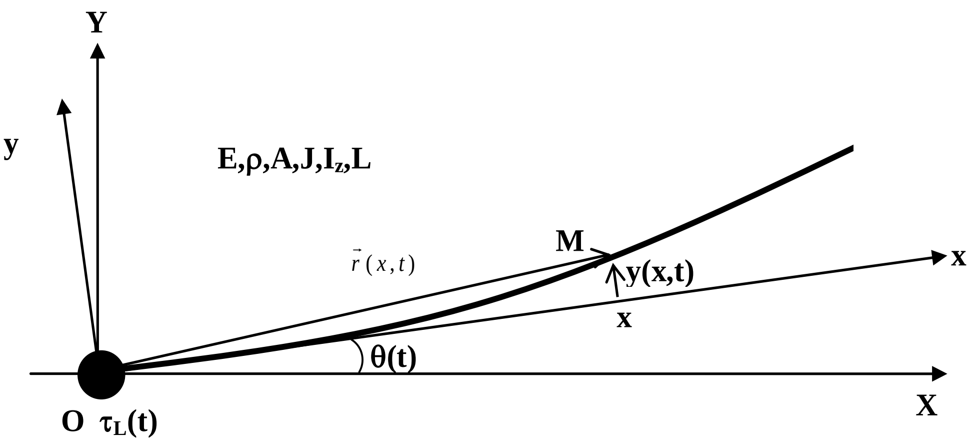

Figure 1. Flexible Arm Coordinates

$\tau_L(t)$ is the motor torque. The position vector of a point M in the rotating coordinate system is $\vec{r}(x,t)$. The deformation of the arm at the point M is $y(x,t)$ and $\theta(t)$ denotes the motor angular position.

The system parameters are summarized in the following table:

Table 1. System Parameters

Parameter	Symbol	Value
Length	L (cm)	41.9
Density	ρ (Kg/m^3)	7756
Young's modulus	E (GPa)	193
Moment of area	I_z (m^4)	1.6710 $^{-12}$
Section	A (mm x mm)	20 x 1
Motor resistance	R_m (Ω)	2.6
Motor inductance	L_m (mH)	0.18
Motor gain	k_m ($V/(rad.s^{-1})$)	7.6810^{-3}
Speed reduction factor	k_g	70
Motor performance	η_m	0.69
Performance of the speed reducer	η_g	0.9
Moment of inertia	J (kg. m^2)	2.08 10^{-3}
Damping factor	b ($N\ m/rad.s^{-1}$)	4.10 $^{-3}$

The displacement of point M with respect to the absolute reference frame is given by:

$$Y = y(x,t) + x\ \theta \quad (1)$$

The deformation $y(x,t)$ is expressed by a finite sum of shape functions weighted by the generalized coordinates [1]:

$$y(x,t) = \sum_{i=1}^{n} q_i(t)\,\phi_i(x) \tag{2}$$

where n is the number of vibration modes, q_i is the ith generalized coordinate and $\phi_i(x)$ denotes the ith shape function. The polynomial functions,

$$\phi_i(x) = (\frac{x}{L})^{i+1},$$

are used in the discretization of the deformation [14].

In this work, only the first two vibration modes are considered so that:

$$Y = x\theta + q_1\phi_1 + q_2\phi_2 \tag{3}$$

$$\vec{v} = (x\dot{\theta} + \dot{q}_1\phi_1 + \dot{q}_2\phi_2)\,\vec{j} \tag{4}$$

The model of the arm is obtained by writing the equations of Lagrange:

$$\frac{d}{dt}(\frac{\partial \ell}{\partial \dot{q}_i}) - \frac{\partial \ell}{\partial q_i} + \frac{\partial R}{\partial \dot{q}} = F_i \tag{5}$$

where q_i is the ith coordinate of the vector Q = [θ, q_1, q_2]^T, *Fi* denotes the generalized force associated with q_i and $l = T - V$ is the *Lagrangian* of the system.

The kinetic energy T is given by:

$$T = \frac{1}{2}J\dot{\theta}^2 + \frac{1}{2}\rho A\int_0^L \vec{v}^T\vec{v}\,dx \tag{6}$$

The potential energy V is:

$$V = \frac{1}{2}EI_z\int_0^l \left[\frac{\partial^2 Y}{\partial x^2}\right]^T \left[\frac{\partial^2 Y}{\partial x^2}\right]dx \tag{7}$$

The Rayleigh dissipation function is expressed by:

$$R = \frac{1}{2}b\dot{\theta}^2 + \frac{1}{2}EI_z\kappa_e\int_0^l \left[\frac{\partial^2 Y}{\partial x^2}\right]^T \left[\frac{\partial^2 Y}{\partial x^2}\right]dx \tag{8}$$

where κ_e is the internal damping coefficient of the arm we will neglect according to our assumptions.

Written in a matrix form, the model of the arm becomes:

$$M\ddot{Q}(t) + H\dot{Q} + KQ(t) = F(t) \tag{9}$$

where:

$$M = \begin{bmatrix} J + \frac{\rho AL^3}{3} & \frac{\rho AL^2}{4} & \frac{\rho AL^2}{5} \\ \frac{\rho AL^2}{4} & \frac{\rho AL}{5} & \frac{\rho AL}{6} \\ \frac{\rho AL^2}{5} & \frac{\rho AL}{6} & \frac{\rho AL}{7} \end{bmatrix}, \quad K = \begin{bmatrix} 0 & 0 & 0 \\ 0 & \frac{4EI_z}{L^3} & \frac{4EI_z}{L^3} \\ 0 & \frac{4EI_z}{L^3} & \frac{4EI_z}{L^3} \end{bmatrix}, \quad H = \begin{bmatrix} b & 0 & 0 \\ 0 & 0 & 0 \\ 0 & 0 & 0 \end{bmatrix}, F(t) = \left[\tau_L, 0, 0\right]^T$$

2.2. Servomotor Modeling

The dynamic equations of the DC actuator are given by:

$$\begin{aligned} v_m &= R_m i_m + L_m \frac{di_m}{dt} + k_m \omega_m \\ J\frac{d\omega}{dt} &= \tau_L - b\omega \\ \tau_m &= \eta_m k_m i_m \\ \tau_L &= \eta_g k_g \tau_m \\ k_g &= \frac{\omega_m}{\omega} \\ \omega &= \dot{\theta} \end{aligned} \tag{10}$$

where ω_m and ω denote speed respectively before and after the speed reduction, τ_m and τ_L are torque respectively before and after speed reduction, v_m is the motor voltage and i_m denotes the motor current.

Neglecting the electrical time constant L_m/R_m with respect to the mechanical time constant J/b, the model of the actuator becomes:

$$\frac{\theta(s)}{V_m(s)} = \frac{Am}{s(s+\omega_{0m})} \tag{11}$$

where $A_m = \frac{\eta_m n_g k_m k_g}{R_m J}$ and $\omega_{0m} = \frac{b}{J} + \frac{\eta_m n_g k_m^2 k_g^2}{R_m J}$.

2.3. Global System of Equations

The torque τ_L is related to the motor voltage by:

$$\tau_L = \frac{\eta_m n_g k_m k_g}{R_m}(v_m - k_m k_g \dot{\theta}) \tag{12}$$

Using this expression, the model of the arm (Eq. (9)) becomes:

$$M\ddot{Q}(t) + H_1\dot{Q} + KQ(t) = v_m U \tag{13}$$

where $U = \left[\frac{\eta_m n_g k_m k_g}{R_m}, 0, 0 \right]^T$ and $H_1 = \begin{bmatrix} b + \frac{\eta_m n_g k_m^2 k_g^2}{R_m} & 0 & 0 \\ 0 & 0 & 0 \\ 0 & 0 & 0 \end{bmatrix}$

Written in a state space form, the global system of equations is:

$$\begin{cases} \dot{x} = A_0 x + B_0 u \\ Y = C_0 x \end{cases} \tag{14}$$

$$A_0 = \begin{bmatrix} 0_{3x3} & I_{3x3} \\ -M^{-1}K & -M^{-1}H_1 \end{bmatrix},\ B_0 = \begin{bmatrix} 0_{3x3} \\ M^{-1}U \end{bmatrix},\ C_0 = \begin{bmatrix} 1 & 0 & 0 & 0 & 0 & 0 \\ L & 1 & 1 & 0 & 0 & 0 \end{bmatrix},$$

$$x = \begin{bmatrix} \theta & q_1 & q_2 & \dot{\theta} & \dot{q}_1 & \dot{q}_2 \end{bmatrix}^T,\ Y = \begin{bmatrix} \theta & Y_{end} \end{bmatrix}^T,\ u = v_m.$$

The quantities to be observed are the hub angle θ and the displacement of the end of arm Y_{end}:

$$Y_{end} = L\theta + q_1 + q_2 \tag{15}$$

3. Vibration Reduction using Sliding Mode Control

3.1. Reference Trajectory

The reference trajectory is selected by setting the following state vector:

$$x_r = \begin{bmatrix} \theta_r(t) & q_{1r}(t) & q_{2r}(t) & \dot{\theta}_r(t) & \dot{q}_{1r}(t) & \dot{q}_{2r}(t) \end{bmatrix}^T \tag{16}$$

The angle θr is selected to be the step response of a first order system, *i.e.*,

$$\dot{\theta}_r = -\frac{\theta_r}{\tau} + \frac{\theta_c}{\tau} \tag{17}$$

where θc is the final position to be reached and τ is the time constant.
Furthermore, to cancel vibrations, we choose:

$$q_{1r} = q_{2r} = 0 \tag{18}$$

The state space equations of the selected reference trajectory can be written:

$$\dot{x}_r = A_r x_r + B_r \theta_c \tag{19}$$

where $A_r = \begin{bmatrix} -\frac{1}{\tau} & 0 & 0 & 0 & 0 & 0 \\ 0 & 0 & 0 & 0 & 0 & 0 \\ 0 & 0 & 0 & 0 & 0 & 0 \\ 0 & 0 & 0 & -\frac{1}{\tau} & 0 & 0 \\ 0 & 0 & 0 & 0 & 0 & 0 \\ 0 & 0 & 0 & 0 & 0 & 0 \end{bmatrix}$ and $B_r = \begin{bmatrix} \frac{1}{\tau} \\ 0 \\ 0 \\ 0 \\ 0 \\ 0 \end{bmatrix}$.

3.2. First Control Law (Certain Model)

To determine the sliding surface, we write first the state model (14) in the canonical basis of governability. The transition matrix P = [P_1 P_2….P_n], n=6, is obtained according to the following recurrent formulae:

$$\begin{cases} P_n = B_0 \\ P_{n-i} = A_0 P_{n-i+1} + a_{n-i} B_0 \end{cases} \tag{20}$$

where i varies from 1 to n-1 and a_i are the coefficients of the following characteristic polynomial:

$$\det(\lambda I - A_0) = \lambda^n + a_{n-1}\lambda^{n-1} + \ldots\ldots\ldots + a_1\lambda + a_0$$

The canonical form of the state model (14) is:

$$\begin{cases} \dot{X} = AX + Bu \\ Y = CX \end{cases} \tag{21}$$

$$X = P^{-1}x, \; A = P^{-1}A_0 P = \begin{bmatrix} 0 & 1 & 0 & 0 & 0 & 0 \\ 0 & 0 & 1 & 0 & 0 & 0 \\ 0 & 0 & 0 & 1 & 0 & 0 \\ 0 & 0 & 0 & 0 & 1 & 0 \\ 0 & 0 & 0 & 0 & 0 & 1 \\ -a_0 & -a_1 & -a_2 & -a_3 & -a_4 & -a_5 \end{bmatrix}, \; B = P^{-1}B_0 = \begin{bmatrix} 0 \\ 0 \\ 0 \\ 0 \\ 0 \\ 1 \end{bmatrix}, \; C = C_0.P$$

The sliding surface s is defined by [7-8]:

$$s = \sigma(X_r - X) + \lambda \int_0^t (\theta - \theta_r)\,dt \tag{22}$$

where $\sigma = [\sigma_0, \ldots\ldots, \sigma_{n-1}]$ and $X_r = P^{-1}x_r$.

The integral part in the previous expression has the effect of canceling the static angle error. s can also be written as:

$$s = \sigma(X_r - X) + \lambda \int_0^t C_r (X_r - X)dt \tag{23}$$

where $C_r = [1 \quad 0 \quad 0 \quad 0 \quad 0 \quad 0]$ P.

Lemma 1: The coefficients λ and σ_i are determined by the desired dynamic.

Proof:

According to (21) and (23):

$$\dot{s} = \sigma(\dot{X}_r - AX - Bu) + \lambda C_r(X_r - X) \quad (24)$$

In the sliding vicinity, $\dot{s} = 0$, i.e.

$$0 = \sigma(\dot{X}_r - AX - Bu_{eq}) + \lambda C_r(X_r - X) \quad (25)$$

u_{eq} is the equivalent control and is given by:

$$u_{eq} = -(\sigma B)^{-1}(\sigma A + \lambda C_r)X + (\sigma B)^{-1}(\sigma \dot{X}_r + \lambda C_r X_r) \quad (26)$$

Using (21) and (26), the sliding dynamic equations become:

$$\dot{X} = A_e X + B(\sigma B)^{-1}(\sigma \dot{X}_r + \lambda C_r X_r) \quad (27)$$

where $A_e = A - B(\sigma B)^{-1}(\sigma A + \lambda C_r)$.

The desired dynamic is determined by selecting appropriate eigenvalues of A_e. Indeed, let A, σ and B be:

$$A = \begin{bmatrix} A_1 \\ A_2 \end{bmatrix}, \quad \sigma = \begin{bmatrix} K_1 & K_2 \end{bmatrix}, \quad B = \begin{bmatrix} 0_{(n-1)x1} \\ 1 \end{bmatrix} \quad (28)$$

where $A_1 \in R^{(n-1)xn}$ and $K_1 \in R^{1x(n-1)}$. The following expression of A_e can be easily derived:

$$A_e = \begin{bmatrix} A_1 \\ 0 \end{bmatrix} - BK_2^{-1}\begin{bmatrix} K_1 & \lambda \end{bmatrix}\begin{bmatrix} A_1 \\ C_r \end{bmatrix} \quad (29)$$

Expression (29) shows that the equivalent dynamic in the sliding vicinity is similar to that obtained in the classical state feedback control where the feedback matrix L is given by:

$$L = K_2^{-1}\begin{bmatrix} K_1 & \lambda \end{bmatrix}\begin{bmatrix} A_1 \\ C_r \end{bmatrix} \quad (30)$$

Choosing the desired dynamic that is the matrix L, the coefficients λ and σ_i are calculated as follows:

$$\begin{bmatrix} K_1 & \lambda \end{bmatrix} = K_2 L \begin{bmatrix} A_1 \\ C_r \end{bmatrix}^{-1} \quad (31)$$

In subsequent sections, K_2 is chosen to be 1 and consequently $\sigma B = 1$.

Sliding control:

The sliding control is given by:

$$u = u_{eq} + M \ sign \ (s) \tag{32}$$

According to (24), (25) and (32):

$$\begin{aligned} s\dot{s} &= s(\sigma(\dot{X}_r - AX - B(u_{eq} + M.sign(s)) + \lambda C_r(X_r - X)) \\ &= s(\sigma(\dot{X}_r - AX - Bu_{eq}) + \lambda C_r(X_r - X)) - s\sigma BM.sign(s) \\ &= -M|s| \end{aligned}$$

To reach the sliding surface with a convergence speed greater than η, M must verify the following condition of attractiveness:

$$M \geq \eta \tag{33}$$

3.3. Second Control Law (Uncertain Model)

In the case of uncertain model where system parameters are not known with enough accuracy or vary with time, we show that we have to increase the discontinuity M to maintain the attractiveness of the sliding surface [7-8].

Suppose that system parameters a_i may vary around their nominal values a_i^* as follows:

$$\left|a_i - a_i^*\right| \leq \delta_i \tag{34}$$

where δ_i denotes the maximum change in the parameter ai (i=0 to n-1).

Replacing A by A + ΔA in (24), and using (25) and (32) give:

$$\begin{aligned} s\dot{s} &= s(\sigma(\dot{X}_r - (A + \Delta A)X - B(u_{eq} + M.sign(s)) + \lambda C_r(X_r - X)) \\ &= s(\sigma(\dot{X}_r - AX - Bu_{eq}) + \lambda C_r(X_r - X)) - s\sigma\Delta AX - \sigma BM.sign(s) \\ &= -s\sigma\Delta A X - M|s| \end{aligned}$$

Let X = [x_1, x_2, …, x_n], thus:

$$s\dot{s} = \sum_{i=0}^{n-1} \Delta a_i x_{i+1} s - M|s| \tag{35}$$

To reach the sliding surface with a convergence speed greater than η, M must verify the following condition of attractiveness:

$$M \geq \eta + \sum_{i=0}^{n-1} \delta_i \left|x_{i+1}\right| \tag{36}$$

The discontinuity M depends not only on changes in parameters but also the amplitudes of the states. This has the effect of amplifying chattering and cause significant fatigue of the actuators sometimes leading to rupture.

Modified Sliding Control:

To maintain the level of discontinuity M unchanged, the following modified sliding control is proposed:

$$u = u_{eq} + KX + M\ sign(s) \tag{37}$$

Lemma 2: We can set discontinuity M at its minimum value η by switching each coefficient ki between two suitable values.

Proof:

Replacing A by A + ΔA in (24), and using (25) and (37) give:

$$s\dot{s} = s(\sigma(\dot{X}_r - (A + \Delta A)X - B(u_{eq} + KX + M.sign(s)) + \lambda C_r(X_r - X))$$

$$= s(\sigma(\dot{X}_r - AX - Bu_{eq}) + \lambda C_r(X_r - X)) - s\sigma\Delta AXs - \sigma BKX - \sigma BM.sign(s)$$

$$= -s\sigma\Delta AX - sKX - M|s|$$

$$= s\sum_{i=0}^{n-1} \Delta a_i x_{i+1} - s\sum_{i=1}^{n} k_i x_i - M|s|$$

$$= \sum_{i=1}^{n} (\Delta a_{i-1} - k_i) x_i s - M|s|$$

To reach the sliding surface with a convergence speed η, we choose M = η and switch the gains k_i between two values m_i and M_i as follows:

$$\begin{cases} k_i = m_i = -\delta_{i-1} & if\ x_i s \le 0 \\ k_i = M_i = \delta_{i-1} & if\ x_i s \ge 0 \end{cases} \tag{38}$$

The implementation of this switching scheme provides a robust control against parameter changes and limited values of the parameter M.

4. Simulation Results

To compare the two previous control laws, SIMULINK models were constructed in both cases. The simulation results were compared in the certain and uncertain cases. In the case of the exact model, the system parameters are supposed to be known exactly and the feedback matrix L is calculated based on the nominal parameters. In the uncertain case, the system parameters are supposed to vary around their nominal values. In this study, the maximum percentage change about the nominal values is 40%; the matrix L is calculated based on nominal parameters. The convergence rate η has been set to 0,001 in all cases.

Figure 2 shows the motor angle θ and the tip deviation in the case of the exact model. The motor angle tracks exactly the reference that is the first order system step response. The comparison between the tip deviations of both the beam ($Y_{beam} = L\theta + q_1 + q_2$) and the rigid body ($Y_{rigid\ body} = L\theta$) shows that the vibration was almost canceled.

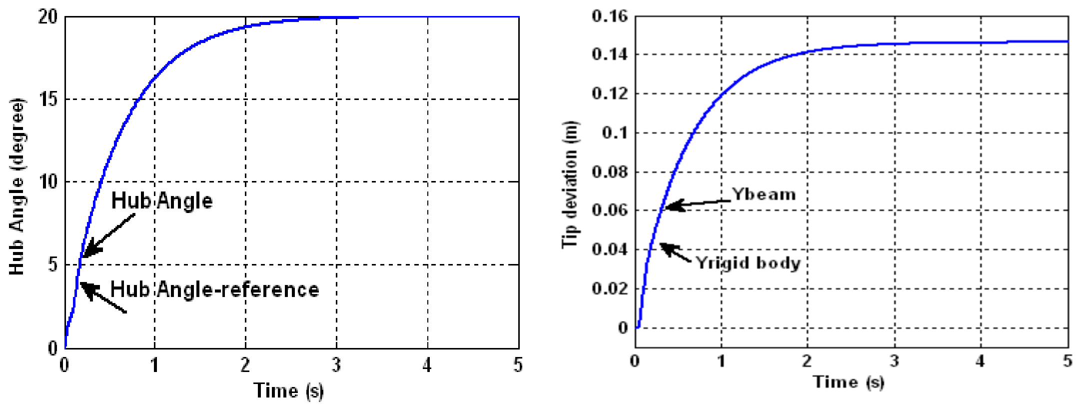

Figure 2. Hub Angle and Tip Deviation M=0.001 (Exact model-1st Control Law)

Figure 3 shows the motor voltage in the cases M = 0.001, 0.1 and 1. We can see the obvious fact that more M increases, the chattering increases.

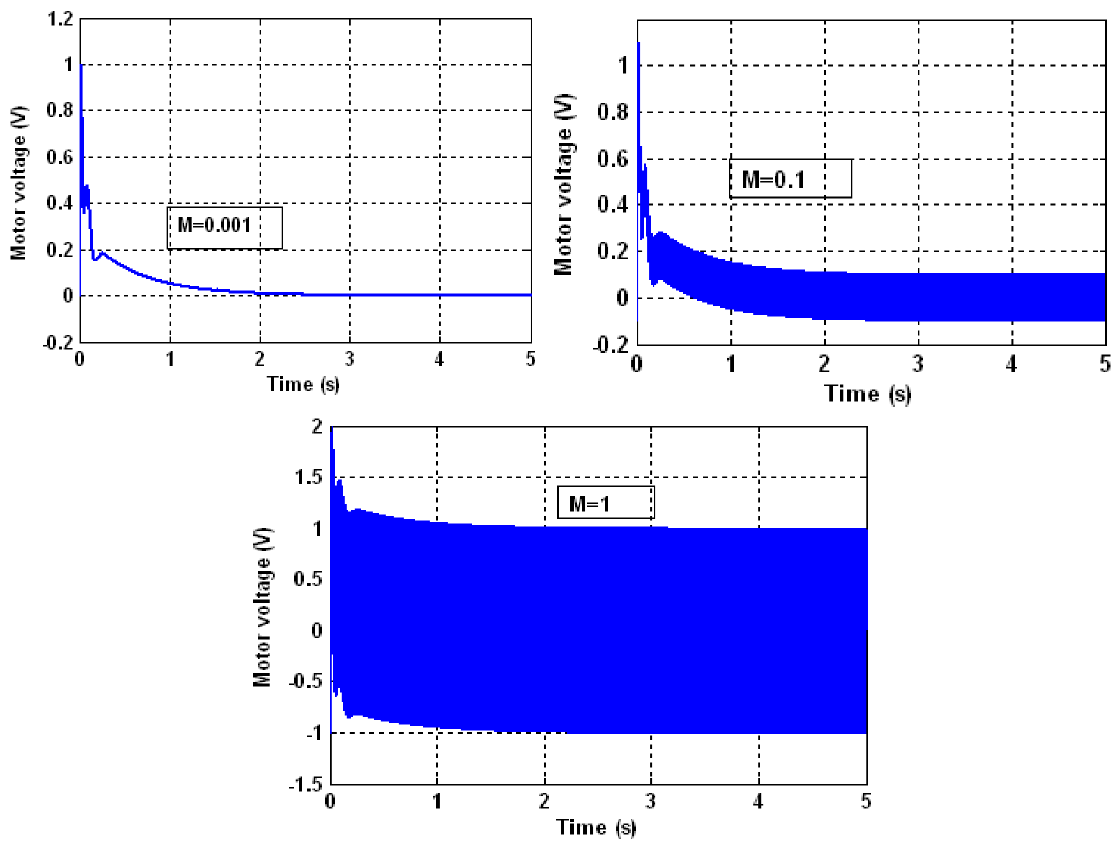

Figure 3. Motor Voltage in the Cases M=0.001, 0.1 and 1 (Exact Model-1st Control Law)

By using the first control law, changing the values of system parameters around their nominal values (Δa_0=-40%, Δa_1=32%, Δa_2=-20%, Δa_3=9%, Δa_4=40%, Δa_5=40%) leads to instability (see figure 4).

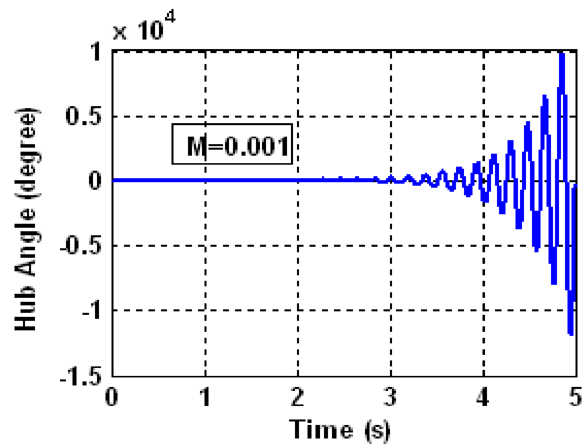

Figure 4. Hub Angle in the Case M=0.001 (Uncertain Model-1st Control Law)

To regain stability, we had to increase M but this amplifies chattering (Figure 5).

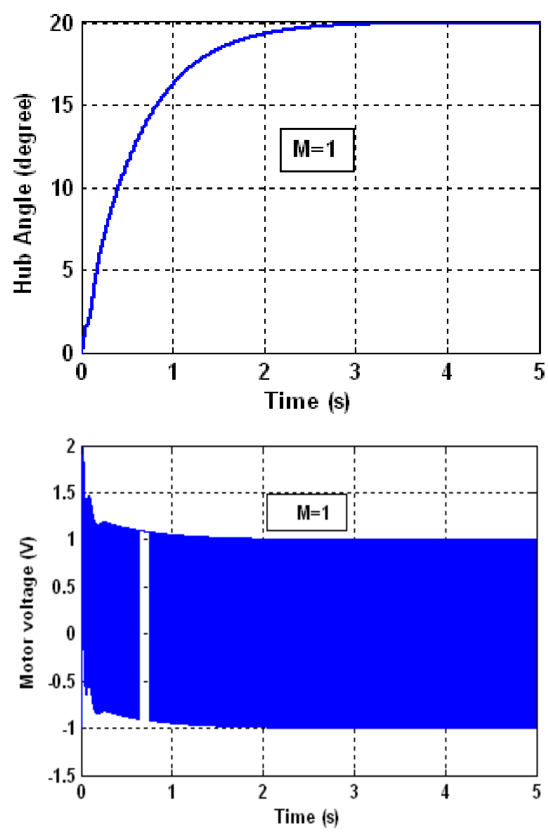

Figure 5. Motor Voltage and Hub Angle in the Case M=1 (Uncertain Model-1st Control Law)

To show the robustness of the second control law, the simulation has been carried out using the same changes in the system parameters. The discontinuity M has been set to its minimum value 0,001. Figure 6 shows that the dynamic response is stable and the chattering has been reduced to an acceptable level. This confirms the effectiveness of the second control law.

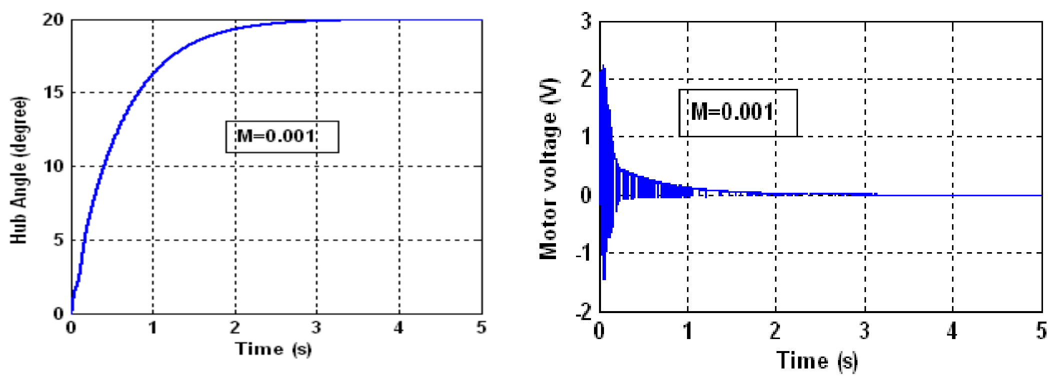

Figure. 6 Motor Voltage and Hub Angle in the Case M=0.001 (Uncertain Model-2nd Control Law)

5. Conclusion

In this paper, simulation results for trajectory tracking and vibration damping of a flexible single link manipulator are presented. The performances of a two proportional-integral sliding mode control schemes are examined for input tracking capability, level of vibration reduction and time response specifications. A comparison of the results shows the effectiveness and robustness of the second control law. The paper gives also more insight into the mathematical development involved in such a design.

Nevertheless, important issues must be resolved to implement the control in practice. First, the full known of the states is required for successful experiments. Data acquisition and observer design is the main issue to resolve before building the test bench. Moreover, it is known that SMC systems are vulnerable to the effects of high-frequency dynamics often neglected in control system design. These neglected elements can be considered equivalent to unstructured uncertainty in the plant model. It is important to know the effects of finite bandwidth actuators/sensors on stability and vibration control. Also, further investigation into the actions to avoid exciting the un-modeled higher frequency dynamics is required.

References

[1] M. Saad, "Robot Manipulators Trends and Development", Edited A. Jimenez and B. M. Al Hadithi, InTech **(2010)**, pp. 73-100.

[2] G. Song and H. Gu, "Active Vibration Suppression of a Smart Flexible Beam Using a Sliding Mode Based Controller", J. Vibration and Control, vol. 13, no. 8, **(2007)**, pp. 1095-1107.

[3] L. M. Capisani, A. Ferrara and L. Magnani, "Design and Experimental Validation of a Second-order Sliding-mode Motion Controller for Robot Manipulators", Int. J. Control, Taylor & Francis Group, vol. 82, no. 2, **(2009)**, pp. 365-377.

[4] D. Kwon and W. Book, "A Time-Domain Inverse Dynamic Tracking Control of a Single-Link Flexible Manipulator, J. Dynamic Systems, Measurement and Control", vol. 116, **(1994)**, pp. 193-200.

[5] M. Bakhti and B. Bououlid Idrissi, "Active Vibration control of a flexible manipulator using model predictive control and Kalman optimal filtering, Int. J. Engineering Science and Technology", vol. 5, **(2013)**, pp. 165-177.
[6] F. Beltran-Carbajal, G. Silva-Navarro, H. Sira-Ramirez and J. Quezada-Andrad, "Active Vibration Control Using On-line Algebraic Identification of Harmonic Vibrations", Proceedings of the American Control Conference, Portland, USA, pp. 4820-4825, **(2005)** June 8-10.
[7] B. W. Dickinson, A. Fettweis, J. L. Massey, J. W. Modestino, E. D. Sontag and M. Thoma, Eds., "Sliding modes in control and optimization", Communications and Control Engineering Series, **(1992)**.
[8] J. Biannic and A. Fossard, "Commande en régime glissant, Techniques de l'Ingénieur", S 7435, **(2005)**.
[9] X. Zhang, H. Su, L. Xiao and J. Chu, "Robust sliding mode control based on integral sliding surfaces", Proceedings of the American Control Conference, vol. 6, **(2005)**, pp. 4074–4077.
[10] Y. Sam, N. Suaib and J. H. S. Osman, "Proportional Integral Sliding Mode Control for the Half-Car Active Suspension System with Hydraulic Actuator", Proceedings of the 8th WSEAS International Conference on Robotics, Control and Manufacturing Technology, Hangzhou, China, **(2008)** April 6-8.
[11] Q. Khan, A. I. Bhatti, M. Iqbal and Q. Ahmed, "Dynamic Integral sliding mode control of SISO uncertain nonlinear systems, Int. J. Innovative Computing", Information and Control, vol. 8, no. 7, **(2012)**, pp. 4621-4633.
[12] G. Bartolini, A. Ferrara and A. A. Stotsky, "Robustness and performance of an indirect adaptive control scheme in presence of bounded disturbances", IEEE Transactions on Automatic Control, vol. 44, no. 4, **(1999)**, pp. 789-793.
[13] J. E. Slotine and W. Li, Editors, "Applied nonlinear control, Prentice-Hall", New Jersey, **(1991)**.
[14] MacMillan, Editor, "Analytical Methods in Vibrations", MacMillan, New York, **(1967)**.

Authors

Mohammed Rachidi, he was born in Boujaâd, Morocco. He received the engineer's degree from Ecole Mohammadia d'Ingénieurs (EMI-Rabat), Morocco, in 1995 and the Master degree from Mohammed V University, Rabat, Morocco, in 2002. His search interested power electronics and control of electrical machines. Since 1997, he has been working at Ecole Nationale Supérieure d'Arts et Métiers (ENSAM-Meknès), Moulay Ismaïl University, Meknès, Morocco, where he is an assistant Professor in the Department of Electromechanical Engineering.

Badr Bououlid Idrissi, he was born in Marrakech, Morocco. He received the Ph.D. degree from Faculté Polytechnique de Mons, Mons, Belgium, in 1997 and the engineer's degree from Ecole Nationale de l'Industrie Minérale (ENIM-Rabat), Morocco, in 1992. Since 1999, he has been working at Ecole Nationale Supérieure d'Arts et Métiers (ENSAM-Meknès), Moulay Ismaïl University, Meknès, Morocco, where he is a Professor in the Department of Electromechanical Engineering, in the areas of power electronics and electrical machines.